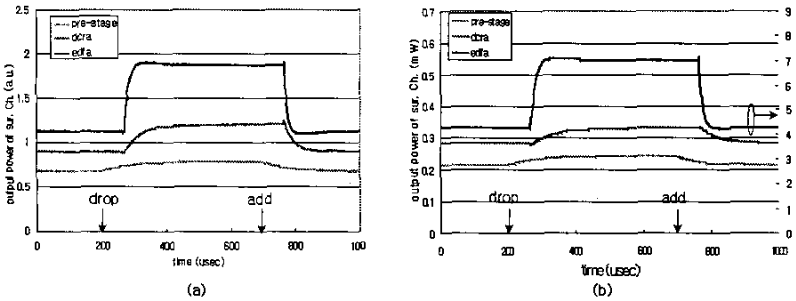

Fig.2. Output power of surviving channel after pre-stage, DCRA, EDFA in each trace when input power of DC-HFA is changed from -2dBm to -5dBm, and vice versa. (a) Experimental results (b) Numerical simulation results

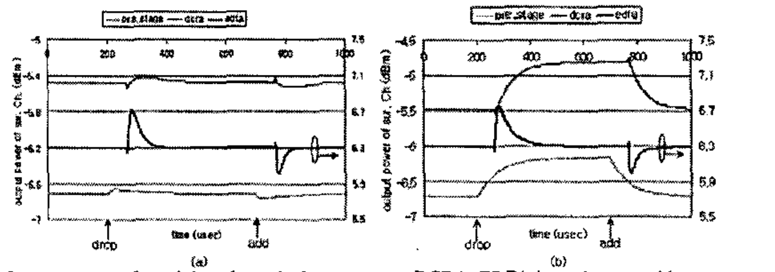

Fig.3. Output power of surviving channel after pre-stage, DCRA, EDFA in each trace with pump power control (a) in each stage (b) in EDFA only

dynamics of EDFA rather than pre-stage and DCRA. The trace after EDFA have the remained feature of fast change in DCRA resulted from Raman-induced crosstalk. The transient response in EDFA is mainly determined by the decay time of Er-ion and the signal, pump powers, while the transient phenomena in DCRA are given by the transit time of DCF.

The dynamics of DC-HFA can be explained with the help of numerical calculation. The models of EDFA's [4] and FRA's [5] to describe the transient dynamics are realized for each stage of DC-HFA. The add-drop of channels is simulated by the change of power in single saturation tone located at the wavelength of 1547nm. Fig.2-(b) shows the results of the transients after each stage of DC-HFA. The results are very similar to the experimental results shown in Fig.2-(a).

4. Gain control in DC-HFA

Because the gain excursions in surviving channel in DC-HFA is quite large and the transient time is fast as 24 μsec due to the high output power in EDFA, the gain control electronics should be very fast to suppress the gain deviation sufficiently. However, the transit time of DCF can be used as the delay time for the control electronics with monitoring the input power of DC-HFA. The gain control in DC-HFA has sufficient time for the control electronics, therefore it can reduce the gain deviation of surviving channel more effectively.

Moreover, because the gain excursion after pre-stage and DCRA are smaller than after EDFA and the transients after pre-stage and DCRA are relatively slower than after EDFA, the gain of surviving channel may be controlled by controlling the pumping power of EDFA only. We compared the transient phenomena when the gain of each stage was controlled separately and only the pump power of EDFA was controlled without controlling in pre-stage and DCRA. The results are demonstrated by the numerical simulation explained in the above.

Figure 3 shows the results of gain control with monitoring the input power of DC-HFA. The gain of each stage is controlled separately in Fig.3-(a), where the pump power is adjusted followed by the change of input power in feed-forward scheme. The delay time of control electronics was assumed to be 5 μsec for the pre-stage, and 68 μsec that corresponds to the transit time of DCF for DCRA and also for EDFA. The gain deviation after EDFA was smaller than +/- 0.4 dB. In Fig.3-(b), the pump power of EDFA only was controlled where the pump power of pre-stage and DCRA had not been changed. The delay time of control electronics was set to be 68 μsec for EDFA. The gain deviation shown in Fig.3-(b) after EDFA is similar as the result of Fig.3-(a). The detailed shapes of transient traces are different from each other, however, output power variation is confined in the range of peak gain excursion. From the results, the pump power control for EDFA only is enough to suppress the gain excursion in DC-HFA.

Because the pump power of pre-stage and DCRA are set to be constant in this gain control method, the gain of pre-stage and DCRA is larger after dropping channels than the gain with fully loaded channels. The pump power of EDFA in Fig.3-(b) is lower than the pump power in the case of Fig.3-(a). Therefore, the noise figures of the surviving channels after dropping channels are better than before in the gain control method of controlling EDFA only. The pump power level to control the gain of DC-HFA is easily found experimentally. The gain and noise figure after dropping channels with the pump power conditions will be discussed in the presentation.

5. Conclusions

The transient effects resulted from the add-drop of channels in DC-HFA are experimentally observed. The dynamic response of DC-HFA is governed by the transients of EDFA because it has the fastest response time. The transient effects are well explained with the numerical models to describe the dynamics of EDFA's and FRA's. The gain control method to adjust the pump power of EDFA only is demonstrated by the numerical simulation. The scheme has the advantages that there is enough time delay for the control electronics due to the transit time of DCF, and the surviving channels have the lower noise figure after dropping channels.

6. References

[1] Y. Emori, Y. Akasaka, and S. Namiki, "Less than 4.7dB noise figure broadband in-line EDFA with a Raman amplified -1300ps/nm DCF pumped by multi-channel WDM laser diodes," OAA'98, 72-77 (1998)

[2] W.Y. Oh, S.S, Lee, H. Lee, and W. Seo, "16-channel C-band hybrid fiber amplifier comprising an EDFA and a single diode laser pumped dispersion compensating Raman amplifier," ECOC2000, 4.4.5 (2000).

[3] S. Gray, "Transient gain dynamics in wide bandwidth discrete Raman amplifiers," OFC2002, ThR2 (2002).

[4] E. Desurvire, "Erbium-doped fiber amplifiers," John Wiley & Sons, Inc. (1994).

[5] C. Chen and W. S. Wong, "Transient effects in saturated Raman amplifiers", Electron. Lett. 37, 371-373 (2001).

ThC 3 **9:00 AM**

Transient Gain Dynamics in Saturated Raman Amplifiers with Multiple Counter-Propagating Pumps

A. Bononi, M. Fuochi, *Dept. di Ingegneria dell'Informazione, Parma, Italy, Email: bononi@tlc.unipr.it.*

A new block diagram of Raman amplifiers with multiple backward pumps is proposed, for use in commercial simulators. Transient computation times are shorter by more than an order of magnitude as compared with the full solution of the propagation equations.

Introduction

The need to enlarge the optical transmission bandwidth to increase system capacity has favored the development of multi-pumped Raman amplifiers due to their large amplification bandwith with reduced gain ripple and low noise figure [1]. Gain transients due to sudden channel add/drop, or to burst-mode transmission as in IP-over-WDM, have been shown to exist even in saturated Raman amplifiers [2]. A simple system model for the saturated Raman amplifier with single backpropagating pump has been introduced in [3]. Such model, based on the solution of a single update equation for the pump depletion, allows drastic savings in gain transient computation times when a large number of time-varying wavelength division multiplexed (WDM) channels feed the amplifier, with very little accuracy degradation, as long as the signal-induced pump depletion remains below 30 % [3].

This paper extends the model in [3] to the multiple backpropagating pumps case, thus providing a valuable tool for the fast computation of both transient and steady-state amplifier response. We give a block-diagram scheme of the amplifier, which could be implemented in any commercial simulator, much as with Erbium amplifiers [4]. We apply the model to two realistic case studies, showing the accuracy of the model and discussing its limitations.

Model

Suppose M pumps propagate backwards in a fiber of length L at speed v and N WDM signals propagate forward at the same speed v. By casting the propagation equations in the signals and pumps retarded time frames, and solving the propagation equations by neglecting amplified spontaneous Raman scattering (ASRS), signal double Rayleigh backscattering (DRB), and direct signal-signal Raman crosstalk as in [2], we obtain the following expression for the output signal powers:

$$S_j^{out}(t) = S_j^{in}(t) e^{-\alpha_j L} e^{\sum_{p=1}^{M} g_{jp}(1-x_p(t))}$$

$$j = 1,..,N \qquad (1)$$

where α_j is the attenuation of the j-th channel, $S_j^{in}(t)$ the input signal power;

$$g_{jp} = \gamma_{jp} \int_0^L \overline{P}_p(z')dz'$$

where γ_{jp} is the Raman gain coefficient [$W^{-1}km^{-1}$] for signal at wavelength λ_j and pump at λ_p, and

$\overline{P}_p(z)$

the unsaturated steady-state pump profile file and $x_p(t)$ is the *p-th pump depletion.* The M *unknown* pump depletion variables $x_p(t)$ are found by solving the following implicit system of M coupled equations:

$$x_p(t) = \sum_{j=1}^{N} S_j^{out}(t) \otimes h_{jp}(t), \quad p = 1,..,M \tag{2}$$

where ⊗ denotes convolution, and the filter impulse response is

$$h_{jp}(t) = \frac{\lambda_{jp}\lambda_j/\lambda_p}{d\,G_j(L)} \frac{\left[\int_0^{L-\frac{t}{d}} \bar{P}_p(z')G_j\left(z'+\frac{t}{d}\right)dz'\right]}{\left[\int_0^L \bar{P}_p(z')dz'\right]} \cdot \Pi\left(\frac{t-dL/2}{dL}\right) \tag{3}$$

where

$$G_j(L) = \exp\left(-\alpha_j L + \sum_{p=1}^{M} g_{jp}\right)$$

is the unsaturated gain at λ_j, $d=2L/v$ the walkoff parameter, and $\Pi(t)$ the gate function, equal to 1 for $-0.5 \le t \le 0.5$, and zero otherwise.

In summary, the procedure to solve the gain transient problem is the following:

i)compute the pump evolution along z,

$$\bar{P}_p(z)$$

in the absence of signals. This implies solving the steady-state propagation equation for pumps only, accounting for pump-pump power transfer;

ii)compute the MN filter responses, as per (3);

iii)iteratively solve the implicit system of update equations for pump depletions (2).

In essence, the procedure amounts to calculating the steady-state amplifier *bias point* without saturating signals (points i) and ii)), and then evaluating the time-varying signal-induced pump depletions from such bias point. Clearly, since the method makes a fundamental distinction between signals and pumps, schemes in which such distinction is blurred, such as resonant Raman pumping schemes, may not be accurately reproduced by our method.

It is interesting to note that our model can be described by the input-output block diagram shown in Fig. 1, and therefore implemented in commercially available block-diagram simulators [4].

In the scheme, we have also introduced further functional blocks: 1) the RIN filters $h_p^{RIN}(t)$, $p=1,...,M$ [5], which take into account the (possibly present) relative intensity noise (RIN) or modulation on each pump; 2) the pre-emphasis gain blocks $Tilt_j$ $j=1,...N$, [6] which are used as a simple approximate way to account for the power tilt in the signals bandwidth due to direct Raman crosstalk, which can be significant in distributed Raman amplifiers.

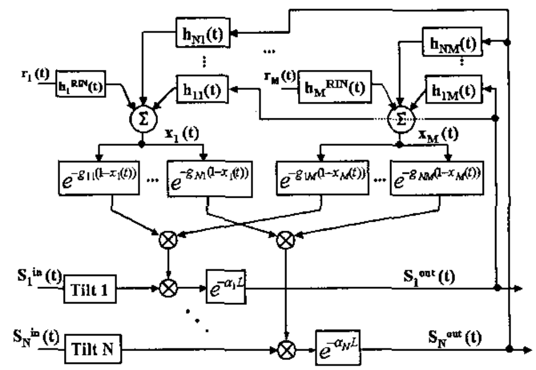

Fig. 1 Block diagram Raman amplifier with M counter propagating pumps and N WDM input signals.

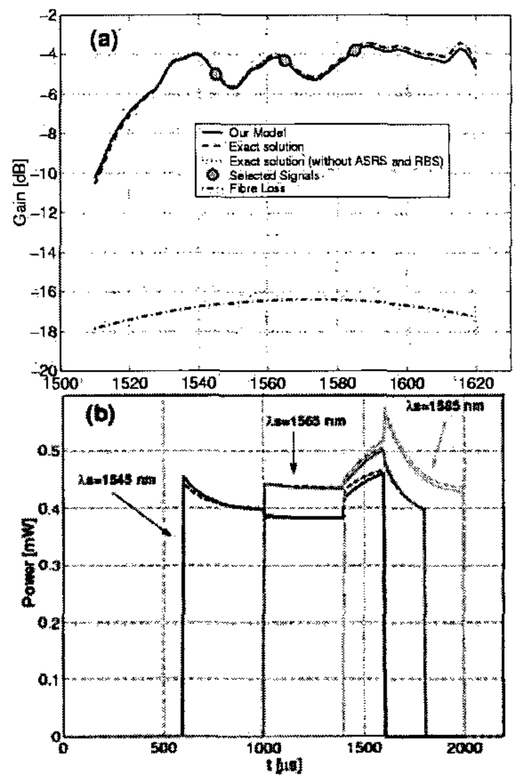

Fig. 2 Distributed multi-pumped Raman amplification in a 80 km NZDF: (a) Raman saturated steady–state gain and fiber loss profile and (b) output power time evolution of channels at 1545, 1565, 1585 nm.

Numerical results

We applied our model to two recently proposed Raman amplifiers, to test their dynamic behavior in deep saturation in order to get a realistic idea of the accuracy of our method.

A) We first consider the distributed amplifier presented in [7], which has an 80 km non-zero dispersion fiber (NZDF) with backpropagating pumps at 1423, 1443, 1464 and 1465 nm, with total input power of 590 mW. We consider the amplification of 80 WDM signals in the [1520, 1610] nm band, with 0 dBm/ch input power, which drive the amplifier in deep saturation.

In Fig. 2(a) we show the *steady-state* gain versus wavelength. The solid line shows the prediction of our model, the dashed line the exact solution of the complete propagation equations, and the dotted line the same exact solution but neglecting ASRS and DRB. The fiber loss profile across the channels is also shown in dash-dotted line. We note that in such heavily saturated amplifier ASE and DRB are negligible, and our model very well matches the exact solution, the error with respect to the complete solution being less than 0.5 dB across the whole bandwidth, and mostly due to the approximations in the *Tilt* blocks [6]. When compared to the unsaturated gain profile [7], one notes a general gain decrease, and a pronounced tilt due both to saturation and to the signal-signal direct Raman interaction. In [7] it was noted that it is possible to change the Raman pumps in order to counteract such direct Raman tilt.

We then ON/OFF modulated all 80 channels with a random pattern and a "slot" duration of T=200 µs, thus emulating packet slotted burst-mode transmission. The time behavior of three selected channels, marked with big dots in Fig. 2(a), is shown in Fig. 2(b), where solid line curves are the output of our model, while dotted lines are the output of the complete time-dependent propagation model (which neglects ASRS and DRB). We note sharp transients across the packets, which indicate a markedly saturated dynamic regime. To give an idea of the execution time savings, running the computations in Matlab on an 800 MHz Pentium V took 2 minutes for our model to both compute the steady-state profile and the transient behavior, while it took over 2 hours for the complete solution of the propagation equations.

B) We next consider the discrete Raman amplifier presented in [8], which has a 5 km dispersion compensating fiber (DCF) with 6 backpropagating pumps at 1428, 1445, 1467, 1484, 1491 and 1507 nm, with total injected power equal to 968 mW. We consider 24 input WDM signals in the range [1530, 1610] nm, with –4.5 dBm/ch input power, as in [8].

Fig 3(a) again shows the steady-state gain, and we note a better match between model and exact solution as compared with the distributed amplifier, because of the absence of direct Raman tilt. We then applied random ON/OFF modulation to all 24 channels with the same period of 200 µs per slot, and the time behavior of the 3 selected channels marked in Fig 3(a) is shown in Fig. 3(b). From the figure, it is clear that the amplifier is deeply saturated, and the match of our model with the exact solution is quite satisfactory, with the largest dynamical error being smaller than a few percent, and occurring at steady-state.

As for the computation times, our model took around 1 minute to run both the static and

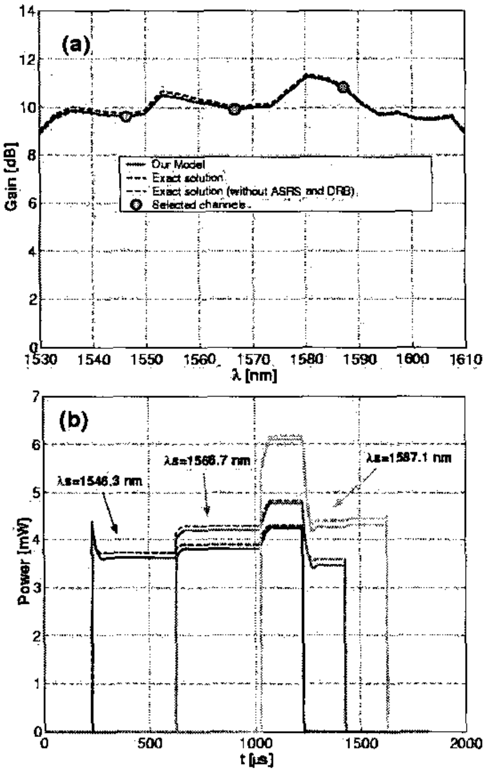

Fig. 3 Discrete multi-pumped Raman amplification in a DCF with length 5.5 km: (a) Raman saturated steady–state gain (b) output power time evolution of channels at 1546.3, 1566.7, 1587.1 nm.

dynamic simulation, while the exact static and dynamic solutions took about 15 minutes. Such shorter time, obtained by keeping the same time resolution as that of the example A), is due the fact that the amplifier is shorter, and the number of channels is smaller. Please note that the savings of our analytical model become more evident when the channel count is larger.

Conclusions
We proposed a new block diagram description of the backward pumped Raman amplifier with multiple pumps, which could be used in commercially-available block diagram simulators, and tested its validity in two realistic case-studies. We found that the proposed model, which neglects ASRS and DRB saturation, yields gain values with an accuracy better than half a dB across the whole bandwidth of a distributed Raman amplifier, while its precision increases in lumped Raman amplifiers. The model computation times for transient gain dynamics are always shorter by more than an order of magnitude as compared with the full transient solution of the propagation equations, the gain becoming more evident for large WDM channel count.

References
[1] S. Namiki and Y. Emori, "Ultra-broadband Raman amplifiers pumped and gain-equalized by wavelength division multiplexed high power laser diodes," *IEEE J. Sel. Topics Quantum Electron.*, vol. 7, pp. 3-16, 2001.
[2] C.J. Chen, and W. S. Wong, "Transient effects in Raman optical amplifiers," in *Proc. OAA 2001*, paper OMC2, 2001.
[3] A. Bononi and M. Papararo, "Transient gain dynamics in saturated counter-pumped Raman amplifiers," in *Proc. OFC 2002*, paper ThR1, pp. 511-512, 2002.
[4] S. Novak, and R. Gieske "Simulink model for EDFA dynamics applied to gain modulation," *IEEE J. Lightwave Technol.*, vol. 20, pp. 986-992, 2002.
[5] C.R.S. Fludger *et al.*, "Pump to signal RIN transfer in Raman fiber amplifiers," *IEEE J. Lightwave Technol.*, vol. 19, pp. 1140-1148, 2001.
[6] A. Bononi, M. Papararo and A. Vannucci, "Impulsive pump depletion in saturated Raman amplifiers," *Electron. Lett., vol.* 37, 886-887, 2001.
[7] C.R.S. Fludger, V. Handerek, R.J. Mears, "Ultra-wide bandwidth Raman amplifiers," in *Proc. OFC 2002*, paper TuJ3, pp. 60-62, 2002.
[8] L. Grüner-Nielsen *et al.* "Module for simultaneous C+L-band dispersion compansation and Raman amplification" in *Proc. OFC 2002*, paper TuJ6, pp. 65-66, 2002.

ThC 4 **9:15 AM**

Nonlinear Inter-Channel Cross Talk of Linear Optical Amplifier (LOA) in DWDM Applications

Y. Awaji, J. Inoue, H. Sotobayashi, F. Kubota, *Communications Research Laboratory, Tokyo, Japan;* T. Ozeki, *Sophia University, Tokyo, Japan, Email: yossy@crl.go.jp.*

We investigated the third order nonlinear effect of linear optical amplifier (LOA) under the condition of amplification of 8ch*10Gb/s WDM signals. We observed the remarkable inter-channel cross talk caused by FWM in the saturated region.

Introduction:
Recently, many attractive optical amplifiers were developed for WDM solution. Erbium doped tellurite fiber amplifier (EDTFA) has broad gain region from C to L band [1]. Bismuth co-doped erbium-doped fiber amplifier (EDFA) is well known as gain-flattened and short length EDFA [2]. On the other hand, erbium doped waveguide amplifier (EDWA) shows the possibility of size-reducible amplifier for optical integrated circuits [3].
A single-chip linear optical amplifier (LOA) was sensationally presented at OFC2001 [4]. It has constant gain for different signal power and amplifies the signal linearly. The gain transient is remarkably low compared to EDFA and semiconductor optical amplifier (SOA) because the carrier population was saturated along the entire length of amplifier. As a result, the inter-channel cross talk caused by gain transition was negligible. Moreover, the dimension of LOA were very small, typically 1 mm x 0.5 mm x 0.15 mm, like as SOA. On the other hand, the gain flatness was very good [5]. Thus, LOA seems to be ideal optical amplifier except output power (~ +13 dBm typically).
However, the information of nonlinearity is lacking. We want to know the limitation of LOA, especially for high power region, and to offer appropriate operation condition based on system requirement. We investigated mainly third order nonlinear effects in LOA. We observed the generation of four-wave mixing (FWM) light and inter-channel cross talk caused by FWM when 8ch * 10 Gb/s WDM signals were amplified. We believe that our report is beneficial for LOA to cooperate with WDM networks.

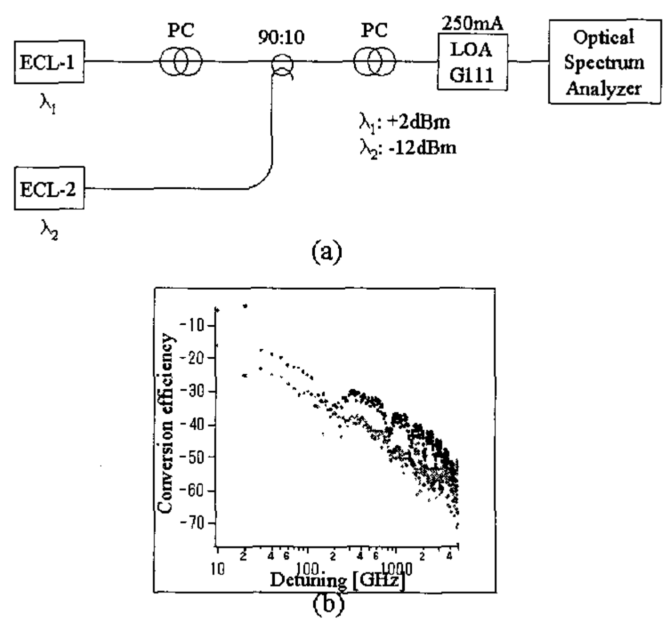

Fig. 1. FWM observation (a) Setup ECL: External-Cavity Laser, PC: Polarizarion Controller
(b) Black circle: Up-conversion, Gray circle: Down-conversion